Preferential Mineralization of $CaCO_3$ Layers on Polymer Surfaces from $CaCl_2$ and Water-Soluble Carbonate Salt Solutions Supersaturated by Poly(Acrylic Acid)

Takashi Iwatsubo, Kimio Sumaru, Toshiyuki Kanamori, Tomohiko Yamaguchi, Toshio Sinbo

National Institute of Advanced Industrial Science and Technology, Central 5, 1-1-1 Higashi, Tsukuba, Ibaraki 305-8565, Japan

Received 23 June 2003; accepted 26 September 2003

ABSTRACT: $CaCO_3$ was mineralized from solutions supersaturated only by poly(acrylic acid) (PAA), without bubbling any CO_2 gas in the solution. For example, a layer of $CaCO_3$ was built up on the surface of a chitosan membrane from a supersaturated aqueous solution containing $CaCl_2$, Na_2CO_3, and PAA. In this newly developed method, the PAA alone suppresses the precipitation of $CaCO_3$ from the bulk solution, and therefore, increases the supersaturated concentration. This concentration is estimated to be the same order as that attained in the method in which both CO_2 gas and PAA were used. At the same time, PAA supplies nucleation fields by forming a polymer complex with chitosan. The crystal system obtained was different from those obtained when using CO_2 gas. Self-organization of aragonite crystallites led to the formation of uniform, concentric, or branching patterns in the surface-domain structure. These patterns had morphologies similar to those discovered by other researchers, typically in the crystallization of ascorbic acid. Thicker layers of $CaCO_3$ could be formed on chitosan membranes, the surfaces of which had been converted to a polyelectrolyte complex (PEC) by exposure to PAA solution before the onset of mineralization. Under certain conditions, the $CaCO_3$ layer had a small spherical curvature, similar to a half-lens, and generated Newton's ring pattern from the interference fringes of visible light. © 2004 Wiley Periodicals, Inc. J Appl Polym Sci 91: 3627–3634, 2004

Key words: biomineralization; membranes; phase diagrams; polyelectrolytes; self-organization

INTRODUCTION

The crystals of $CaCO_3$ formed in many kinds of organisms are regularly assembled and combined with organic polymers such as polypeptides or polysaccharides. The structure of pearl consists of aragonite crystals periodically and regularly stacked with chitin and rigid protein as binders.[1] The unique luster of pearls is brought about by multiple reflections and interference of visible light, caused by the stacking structure. The organic–inorganic composite materials of sea urchin skeletal elements overcome the brittleness intrinsic to calcite $CaCO_3$ and possess rupture-resistant properties despite their relatively low density. If such composite materials can be artificially manufactured by mimicking biomineralization, they could be used as lightweight reinforced materials or as biocompatible materials. Moreover, if the composite structure can be regularly controlled on the microscale or the nanoscale, their material properties will surpass those of natural biomineralized composites. Nowadays, aiming at the construction of such materials as a prospective target, biomineralization-mimicking materials and processes for their construction are widely investigated by many researchers.

Kato et al. developed a method for $CaCO_3$ mineralization, in which $CaCO_3$ is generated preferentially on a polymer substrate, with no precipitation from the bulk liquid phase. The supersaturation of $CaCO_3$ was accomplished by Kitano's method in which CO_2 gas was blown into the heterogeneous mixture of $CaCO_3$ powder and water, with stirring.[2] After removal of undissolved excess $CaCO_3$ by filtration of the supersaturated suspension, a polyelectrolyte, such as poly(acrylic acid) (PAA), was dissolved in the supersaturated solution to suppress the precipitation of $CaCO_3$ from the liquid phase. Kato et al. elucidated the effects of the polymer substrate and the species and concentration of the polyelectrolyte on the polymorphism of the $CaCO_3$ crystals obtained, and the size and shape of their surface domains.[3–6] In their method, the polyelectrolyte promotes the nucleation of $CaCO_3$ by combining with a substrate polymer as revealed from X-ray photoelectron spectroscopy (XPS) analysis conducted by Zhang and Gonsalves.[7] At the same time,

Correspondence to: T. Iwatsubo (t-iwatsubo@aist.go.jp).

Contract grant sponsor: Budget for Nuclear Research of the Ministry of Education, Culture, Sports, Science, and Technology of Japan.

Journal of Applied Polymer Science, Vol. 91, 3627–3634 (2004)

polyelectrolytes contribute, to some extent, to an increase in the supersaturation concentration, because they normally decrease the activities of small ions in aqueous solution.[8]

Akashi et al. developed another method,[9] in which a polymer substrate having ionic groups was dipped alternately in aqueous solutions of, for example, $CaCl_2$ and Na_2CO_3. Repetition of this dipping cycle led to mineralization on or in the polymer substrate. The surface of the composite material obtained had good tissue affinity to rat L-929 bone-marrow cells.

In the method that we report here, the supersaturated solution is prepared with, for example, PAA, $CaCl_2$, and Na_2CO_3 solutions, and the increase in the supersaturation concentration of $CaCO_3$ is achieved by the PAA alone. This method will have an advantage in that the concentration of $CaCO_3$ in the solution can easily be varied by changing the concentration of the salts used. Moreover, the potassium and carbonate salt species and their composition ratio can also be varied, although the ratio was fixed at 1 : 1 in this work. To investigate the possibility of controlling the structure, we focused on the relation between the mineralization conditions and the characteristic structure of the resulting composites.

EXPERIMENTAL

Materials

PAA of a molecular weight (M_w) of 2000 Da (GPC) was purchased from Aldrich Chemical Co., Inc. (Milwaukee, WI). Calcium chloride dihydrate ($CaCl_2 \cdot 2H_2O$), sodium carbonate (Na_2CO_3), and ammonium carbonate [$(NH_4)_2CO_3$] were purchased from Wako Pure Chemical Industries, Ltd. (Osaka, Japan). Poly(vinyl alcohol) (PVA) membranes with 50 μm thickness were supplied by Kuraray Co., Ltd. (Osaka, Japan). Chitosan, with a degree of deacetylation of more than 99%, was purchased from Katayama Chemical (Osaka, Japan). A 1% w/w aqueous solution of chitosan, containing acetic acid in a molar quantity equivalent to that of the chitosan monomer unit, was filtered to remove insoluble materials. The filtered solution was poured onto a flat glass laboratory dish and allowed to evaporate until a solid membrane formed. After drying at room temperature, the membrane obtained was immersed in a 1 : 1 v/v mixture of 1*M* aqueous NaOH and ethanol to remove acetic acid and then thoroughly rinsed with water. The thickness of the dry chitosan membrane was measured by a micrometer at five surface positions and found to be about 33 μm on average.

Mineralization method

There are two variations of this method, the diffusion method and the immersion method. In the former, 100 mL of a solution *A* containing *y* mM of PAA with *x* mM of $CaCl_2$, and 100 mL of a solution *B* containing *y* mM of PAA with *x* mM of $(NH_4)_2CO_3$ or Na_2CO_3 was placed in two separate glass vessels separated by the membrane, which was positioned by a rubber O-ring at each surface. Immediately after the solutions were placed in the vessels, the dissolved ions started to diffuse across the membrane toward the opposite sides.

In the immersion method, each glass vessel, separated by the membrane, was filled with 100 mL of a solution *C*, which was a complete mixture of solutions *A* and *B*. In both methods, the surface area of the membrane exposed to the aqueous solutions was a circle with a radius of 1 cm, and mineralization was conducted at 30°C. Each solution was stirred with a rotor driven by a magnet outside the glass compartment, to ensure ideally mixed phases and a minimal thickness of the aqueous boundary layer at the membrane interface. After mineralization, the membrane was taken out from the glass vessels and gently washed with deionized water.

Material evaluation

The difference in weight of the desiccated membrane before and after the mineralization was taken as being equal to the amount of $CaCO_3$ produced, *M* mg. Because the volume of each solution was 100 mL and the formula weight of $CaCO_3$ was 100, the yield of mineralization process can be simply given by 10 M/x%. This is the reason the amount of products was not given in mg/cm^2 unit. The result of mineralization was observed by digital optical microscopy (OM; Keyence VH-8000) with a halogen lamp as a light source, and by scanning electron microscopy (SEM; Topcon DS-720) of a platinum layer coated on the samples. The crystal system of the $CaCO_3$ obtained was identified by X-ray diffraction (Rigaku Geiger-Flex RAX01) of milled sample of membrane, frozen in liquid nitrogen, and crushed into a powder in a clean agate mortar. Concentrations of Ca^{2+} and Cl^- ions in solutions were measured by an ion meter (TOA Electronics, Ltd., IM-40S). Calibration and measurements were conducted at 30°C by adding 10 vol % of ionic-strength adjuster to the test solution.

RESULTS AND DISCUSSION

Phase diagram

In this method, the concentrations of PAA and calcium and carbonate salts should be restricted within a certain range of the phase diagram (Fig. 1) to obtain solid $CaCO_3$ preferentially at the membrane.

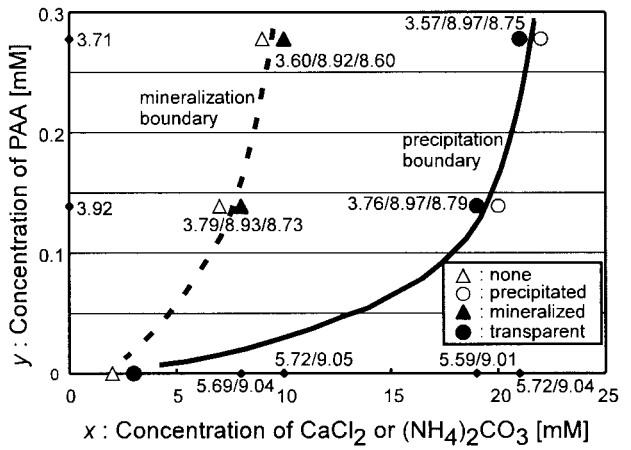

Figure 1 Phase diagram for effective mineralization area. p on the vertical line = pH of PAA solution. a'/b' on the horizontal axis = pH of $CaCl_2$ solution/pH of $(NH_4)_2CO_3$ solution. $a/b/c$ in x– y plane = pH of solution A/pH of solution B/pH of solution C. The concentrations of PAA, $CaCl_2$, and $(NH_4)_2CO_3$ of the solution are represented by the values of y, x, and x, respectively, at the point. For example, p means the pH of PAA solution containing y mM of PAA.

After keeping solution C at 30°C overnight, the existence of precipitation was judged by the naked eye. The presence of a precipitate defines a curve, named the precipitation boundary, in the phase diagram. From OM observation (×450 magnification), the existence of mineralization was checked for samples that had been maintained for almost 2 days under a range of mineralization conditions to the left of the precipitation boundary in the phase diagram. This observation enabled another curve, named the mineralization boundary, to be determined. The pH values of solutions before and after mixing were measured at several points in the phase diagram.

The acidity of PAA suppresses the precipitation of $CaCO_3$, and therefore, elevates the concentrations of Ca^{2+} and CO_3^{2-} in supersaturated solutions. This effect is demonstrated by the precipitation boundary, which meets the abscissa only below 3 mM. The position and shape of this curve change depends on the species of polyelectrolyte, and the calcium and carbonate salts. When samples of PAA having an M_w of 5000, 25,000, or 250,000 Da were used instead of one with an M_w of 2000 Da, the precipitation boundary shifted in the direction of lower salt concentration (data not shown). This phenomenon is explained by a polymer effect on the ionic dissociation of PAA. With PAA of a higher M_w, the dissociation of carboxyl groups will be suppressed, because the high local charge density of the polymer chain demands a high electrostatic energy. Hence, the acidity of high M_w PAA samples will be lower. When the salt concentration is above the boundary value, precipitates from the bulk solution are incorporated into the $CaCO_3$ mineralized at the membrane. This causes difficulties in the evaluation and analysis of the mineralized material. For this reason, the experiments were conducted in the concentration region below the precipitation boundary. In addition, the mineralization boundary is affected by the substrate polymer, as well as by the polyelectrolyte and the calcium and carbonate salts. According to XPS analysis, it was revealed that PAA has been absorbed into chitosan surface layer and formed polyelectrolyte complex (PEC).[7] In this thin PEC layer, the local concentrations of Ca^{2+} and CO_3^{2-} will be elevated up to form the nuclei of $CaCO_3$ by the time-dependent fluctuation of polymer concentration. Because formation of a complex between the substrate polymer and the polyelectrolyte should be necessary for nucleation to occur, a mineralization boundary cannot be defined when formation of a complex does not occur. For example, no mineralization was observed when cellulose acetate membrane was adopted as the substrate.

The comparison of supersaturated concentrations between the present and the CO_2 blowing methods will not be meaningless. Under 1×10^5 Pa of CO_2 gas, saturated concentration of $CaCO_3$ is 7.2 mM at 30°C.[10] On the other hand, the representative Ca^{2+} concentration adopted in the present method is 10 mM, which is of a similar order of magnitude to that in the former method. Therefore, CO_2 blowing will not always be necessary to obtain supersaturated solution. Despite this similarity in Ca^{2+} concentration, the resulting polymorphism was different, as can be seen in the following text.

Polymorphism

X-ray diffraction analyses were made of the products from five different experiments (Table I).

In the absence of PAA, crystallites were precipitated both in the bulk solution and on the membrane. According to OM observations, precipitated crystallites were agglomerated and sedimented on the membrane surface: a calcite crystal system was obtained in this case. Planar growth of the $CaCO_3$ layer was observed under the other four sets of conditions. Mineralization in the presence of PAA led to preferential growth of aragonite structure. Therefore, the complex formation of PAA and chitosan by electrostatic interaction or between PAA and PVA through hydrogen bonding has a marked effect on the structure of the mineralized $CaCO_3$. These resulted polymorphisms contrast with those obtained in the CO_2 supersaturation method, in which calcite and vaterite were formed preferentially on chitosan membranes in solutions containing PAA.[5] Of the polymorphs of $CaCO_3$, calcite is the most stable, and aragonite is formed preferentially in alkaline solutions.[2] Under the last four sets of conditions listed in

TABLE I
Crystal Systems Identified from X-ray Diffraction

Substrate polymer	*y* (mM)	*x* (mM)	Carbonate salt	pH of *C* solution	Time (h)	Method	Weight gain (mg)	Crystal system
Chitosan	0	10	$(NH_4)_2CO_3$	—	164.8	Diffusion	21.6	Calcite
Chitosan	0.139	10	$(NH_4)_2CO_3$	8.70	142.3	Diffusion	20.4	Aragonite
PVA	0.417	20	$(NH_4)_2CO_3$	8.70	137.3	Diffusion	20.6	Aragonite[a]
PVA	0.417	20	$(NH_4)_2CO_3$	8.55	140.5	Immersion	12.1	Aragonite
Chitosan	0.833	20	Na_2CO_3	8.94	139.7	Immersion	13.0	Aragonite

[a] Traces of calcite and vaterite were also found.

Table I, the pH values of the solution ranged from 8.55 to 8.94, which were higher than those observed in the CO_2 supersaturation method,[6] where the pH changed from 6 at the beginning of the experiment to the values between 8 and 9 at the end.[7] Therefore, the difference in pH of initial condition could be responsible for the difference in the crystal system. Also, a coexisting ion, such as Na^+ or excess Ca^{2+}, will affect the polymorphism in the present method.

Self-organization

Aragonite grows fastest in the direction of the *c*-axis, and therefore, its elementary crystallite is a needlelike crystal that, after successive branching by dislocation, takes the overall form of a spherulite (Fig. 2).

In our geometry, nucleation and growth take place preferentially in the polymer complex at the membrane surface. Therefore, the spherulites take the form of disklike domains, in which the *c*-axis lies on the surface, and which grow until they touch each other along hyperbolic boundaries.[11] After contact, the thickness of the $CaCO_3$ layer will increase by a mixture of the following three types of thickening mechanisms: (1) New nucleation takes place, and the disk spreads over the planar domain. (2) The elementary crystal of the domain grows gradually in the direction perpendicular to the *c*-axis. The domain thickness increases. (3) A half-spherulite is generated by three-dimensional branching, and the central region of the domain stands up above the boundary of the domain. As a result, the mineralized $CaCO_3$ layer has a complicated surface structure. Under appropriate conditions, however, the surface structure can have regularity, to some extent. Representative surface morphologies obtained under the conditions (Table II) were examined by OM (Figs. 3–6).

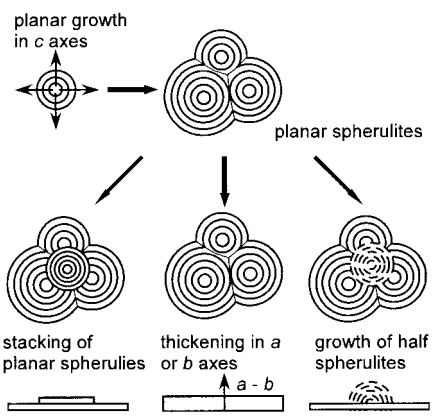

Figure 2 Schematic showing growth process of spherulites on membrane surfaces. The middle panel corresponds to the top view and the bottom panel represents the side view of the system.

Figure 3 shows a domain structure with a uniform density. Figure 4 represents a concentric structure generated in the surface domain. In Figure 5, the concentric structure is modulated along the circumference of the spherulite. In the branching pattern represented by Figure 6, the elementary crystallites have grown to a macroscopic scale, so that branching of the needle crystals is visible.

When viewed through crossed polarization filters, the uniform pattern shows Maltese crosses very clearly, indicating the highest rotational symmetry, even on the scale as fine as the wavelength of visible light. The symmetry declines in Figures 4 and 5, which have less-defined Maltese crosses, and eventually disappears in Figure 6, where the crystallite size was greater than the wavelength of the light. This pattern formation looks similar to the self-organization patterns observed in the crystallization processes of L-ascorbic acid from methanolic solution.[11] The domain of ascorbic acid adopts a uniform pattern at low atmospheric humidity, and a branched pattern under high humidity. The mechanism of formation of the concentric pattern has been inferred theoretically, and the calculated pattern agreed well with experimental results.[11] According to their mechanism, the fluidity of concentrated solutions of ascorbic acid at the surface layer is assumed to be affected by the humidity (high fluidity in high humidity) and to be relevant to the pattern formation. The local crystallization releases solvent that will be absorbed into voids between generated

TABLE II
Conditions for Obtaining Various Domain Structures

Substrate polymer	y (mM)	x (mM)	Carbonate salt	Time (h)	Method	Weight gain (mg)	Domain type
Chitosan	0.139	10	$(NH_4)_2CO_3$	91.7	Diffusion	12.6	Uniform
Chitosan	0.139	10	$(NH_4)_2CO_3$	163.6	Immersion	20.3	Concentric
Chitosan	0.694	13	Na_2CO_3	43.2	Diffusion	0.71	Modulated concentric
PVA	0.277	14	$(NH_4)_2CO_3$	121.7	Diffusion	18.1	Branching

needlelike crystals by capillary force until all the released solvent is absorbed into the voids. Then crystallization starts again at the growth front of domains. The spatial scale and the time scale of the present system correspond to 1/1000 and 10 times, respectively, those of the ascorbic acid system. In the self-organization patterns of the present system, the key factor affecting pattern formation (such as the humidity in the case of ascorbic acid) has not yet been identified. Nevertheless, the mechanism underlying this phenomenon will be similar in both the ascorbic acid system and the present system, because the crystallite of ascorbic acid is a needle that plays an essential role in the formation of a concentric pattern.[11] In the present system, the fluidity of the concentrated ionic solution within the polymer complex surface layer could be responsible for the pattern formation. The interaction of hydrogen bonding between PVA and PAA is weaker than the electrostatic interaction between chitosan and PAA. So the fluidity in the loose structure of PVA and PAA complex layer is higher than that in chitosan and PAA complex layer. This will be the reason our branching pattern resembles the branching pattern of ascorbic acid under high humidity in their appearance.

Surface flatness

Mineralization on a chitosan membrane was conducted by the diffusion method, with $CaCl_2$ and $(NH_4)_2CO_3$ of initial concentrations $y = 0.138$ and $x = 10$, respectively. The diffusion time was 141 h, and the weight of product obtained was 17.3 mg. The domain morphology of this membrane had uniform structure at both sides. Figure 7 shows (a) an transmission image, and (b) a reflection image of the $CaCO_3$ layer obtained. In the latter, interference fringes can be seen on the colorless $CaCO_3$ layer.

This interference is generated by the half-lens configuration of the transparent domains. The conditions for fringes to emerge can be described as follows:[12]

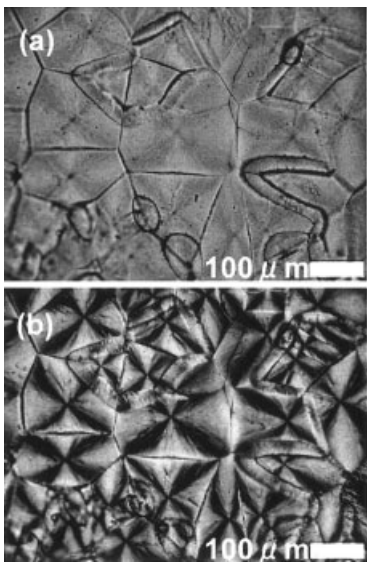

Figure 3 Uniform pattern in domain structure on chitosan membrane: (a) transmission image; (b) transmission image through crossed polarization filters.

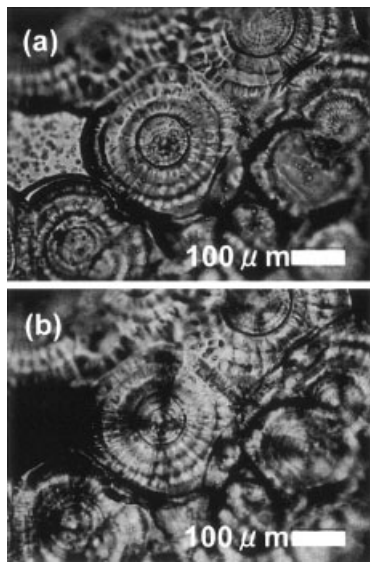

Figure 4 Concentric pattern in domain structure on chitosan membrane: (a) transmission image; (b) transmission image through crossed polarization filters.

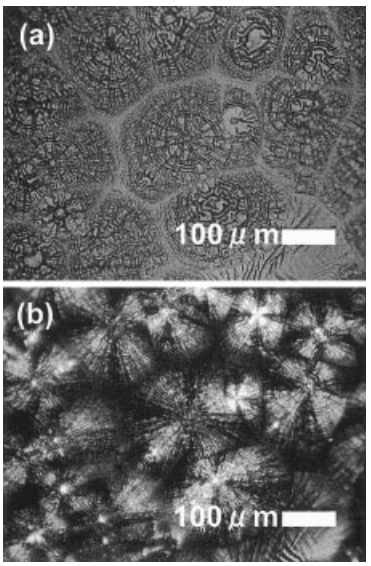

Figure 5 Modulated-concentric pattern in domain structure on chitosan membrane: (a) transmission image, (b) transmission image through crossed polarization filters.

$$2d = m(\lambda/n) \quad \text{light fringe}$$

$$2d = (m + 1/2)\,(\lambda/n) \quad \text{dark fringe}$$

$$m = 0,1,2,\ldots$$

where d is the layer thickness, λ is the wavelength of the light, and n is the refractive index of the crystal layer. Although the light in the present system is not monochromatic, and aragonite has three principal indices, an estimation, taking $\lambda = 500$ nm and $n = 1.6$ as representative values, gives 0.16 μm of a contour for a cycle of fringes. Hence, the height of a typical domain can be estimated as 5 cycles = 0.8 μm, whereas the distance across the domain is 100 μm. These dimensions indicate that the domain surface is relatively flat. In the immersion method, using the same concentrations of PAA, $CaCl_2$, and $(NH_4)_2CO_3$, the domain obtained had no interference fringes, indicating a difference in the mineralization process from that of the diffusion method. To confirm the existence of this difference, mineralization by the diffusion method was examined with several membranes about 33 μm thick, varying the mineralization period. The concentration of Ca^{2+} or Cl^- did not become equal between sides *A* and *B* within 6 days (Fig. 8). Therefore, the existence of a difference between the diffusion process and the immersion process within 6 days was verified.

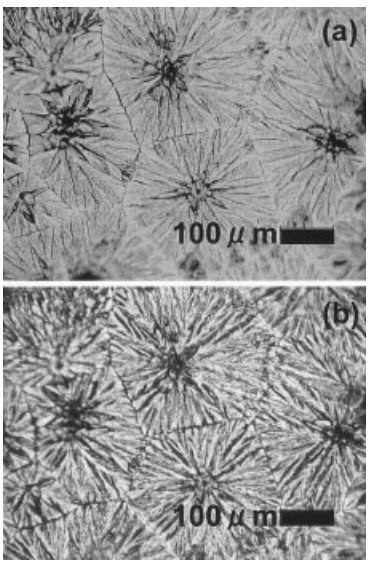

Figure 6 Branching pattern in domain structure on PVA membrane: (a) transmission image; (b) transmission image through crossed polarization filters.

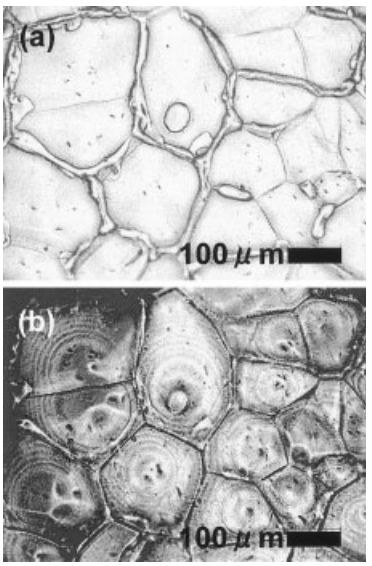

Figure 7 Newton rings formed by the interference of visible light: (a) transmission image, (b) reflection image. 17.3 mg of $CaCO_3$ was obtained in 141.2 h by the diffusion method on chitosan membrane. In monochromatic printing, color separation was conducted and cyan is emphasized to indicate interference fringes.

Measurements by a pH meter showed that the pH of solution *A* became equal to that of solution *B* in less than 1 day (results not shown). From these results, we can speculate that mineralization in this method will proceed by the following path. After the counterdiffusion of ions begins, equality of pH values is reached at a very early stage. Mineralization begins at the membrane surface when the ionic activity product of Ca^{2+} and CO_3^{2-} reaches a certain critical value, which is lower than the value for the corresponding *C* solution. The $CaCO_3$ layer then begins to cover the membrane surface, which in turn causes a decrease in the rate of

diffusive permeation through the membrane. After the surface has become almost covered by the layer, diffusion will take place only through the domain boundaries, and the $CaCO_3$ layer increases in thickness. Consequently, mineralization proceeds more gradually than it does in the immersion method.

Interior mineralization

In the experiments described so far, the nucleation and growth take place initially on the membrane surface, because the polymer complex is formed only at the surface. Then, the $CaCO_3$ layer thickened in an outward direction. If PAA is incorporated in the membrane beforehand, nucleation may take place inside the membrane as well as at the surface or the $CaCO_3$ layer may growth inward as well as outward. To achieve such mineralization, PAA with an M_w of 5000 Da was adsorbed from its aqueous solution onto one side of a chitosan membrane for 1 h at 60°C. This membrane was confirmed to be asymmetric by attenuated total reflectance Fourier transform infrared (ATR–FTIR) analysis, which revealed the formation of a PEC between chitosan and PAA only at the side that was in contact with the PAA solution.[13] For this membrane, mineralization was conducted by the immersion method for 161.1 h, by using 100 mL of solution *A* containing 0.139 mM of PAA with 20 mM of $CaCl_2$, and 100 mL of solution *B* containing 0.139 mM of PAA with 20 mM of $(NH_4)_2CO_3$.

A layer as thick as 15 μm was formed on the side exposed to the PAA solution beforehand, while a thinner layer was formed on the other side (Fig. 9). It is not clear from this observation alone whether the surface layer grew inward or the nucleation occurred in the

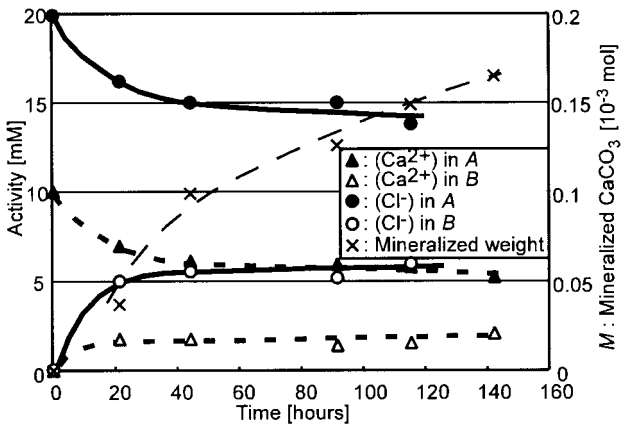

Figure 8 Ionic concentration change during diffusion process with $CaCl_2$ and $(NH_4)_2CO_3$. The initial concentrations were $y = 0.139$ and $x = 10$. Mineralized $CaCO_3$ is expressed in mole unit for the convenience of the comparison to the activity of Ca^{2+}.

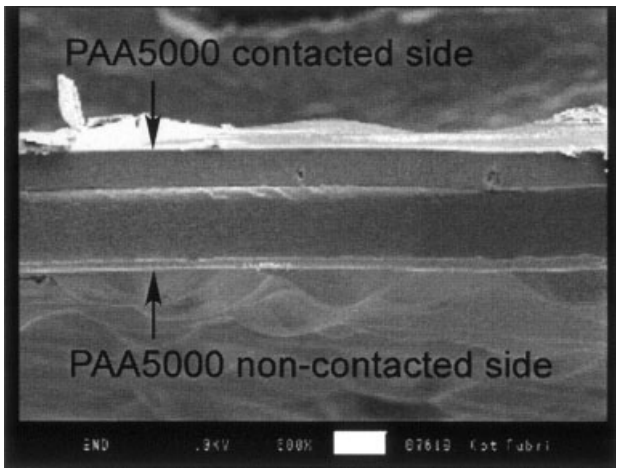

Figure 9 A thick $CaCO_3$ layer is constructed on the side with a preformed PEC of chitosan and PAA. In total, 15.0 mg of $CaCO_3$ was obtained. The white scale bar indicates 16.6 μm.

PEC region inside the membrane and the growth process proceeded until many spherulites contacted each other to form a thick layer. Despite this ambiguousness, the thickness of mineralized layer can be easily controlled, because the extent of PEC formation can be varied, depending on the diffusion time, the temperature, and the M_w of the diffusing polymer in the preincorporation treatment.[13]

CONCLUSION

In the method proposed here, the concentration area effective for preferential mineralization on the polymer membrane was clarified to be bound on the phase diagram by the mineralization and the precipitation boundary curves. The calcium ion was estimated to be the same degree of concentration to that attained in the supersaturation method involving CO_2 gas. In contrast to the CO_2 blowing method, the $CaCO_3$ had a strong tendency to mineralize as aragonite. The domains of these aragonite materials had uniform, concentric, modulated-concentric, or branching morphologies, depending on the specific mineralization conditions. The similarity of these patterns to those found in the crystallization of ascorbic acid implies universality of this phenomenon in crystallization processes. Thickening of the $CaCO_3$ layer not only outward but also inward into the polymer membrane can be achieved by forming a PEC before the onset of mineralization. This method will be useful for producing bulk organic-inorganic composites with improved mechanical properties. Although the optical nature of the $CaCO_3$ layer depends on the direction of the crystal axes of the aragonite, interference fringes can emerge on the surface domains under appropriate conditions in the diffusion method. The present method in which

CO_2 blowing is not employed will have many application fields because the mineralization is not restricted within carbonate salts.

A part of this study was financially supported by the Budget for Nuclear Research of the Ministry of Education, Culture, Sports, Science, and Technology (MEXT) of Japan, based on the screening and counseling by the Atomic Energy Commission.

References

1. Weiner, S.; Traub, W. Philos Trans R Soc London Ser B 1984, 304, 425.
2. Kitano, Y. Bull Chem Soc Jpn 1962, 35 1980.
3. Kato, T.; Suzuki, T.; Amamiya, T.; Irie, T.; Komiyama, M; Yui, H. Supramol Sci 1998, 5, 411.
4. Kato, T.; Amamiya, T. Chem Lett 1999, 3, 199.
5. Hosoda, N.; Kato, T. Chem Mater 2001, 13, 688.
6. Hosoda, N.; Kato, T.; Polym Prepr Jpn 2000, 49, 3991.
7. Zhang, S.; Gonsalves, K. E. Langmuir 1998, 14, 6761.
8. Nagasawa, M.; Kagawa, I. J Polym Sci 1957, XXV, 61.
9. Ogome, D.; Serizawa, T.; Akashi, M. Preprints of the 11th Symposium of Research Group on Polymers and Biosciences 2001, 57 (in Japanese).
10. Stephen, H.; Stephen, T. Solubilities of Inorganic and Organic Compounds; Vol. I; Pergamon Press: Oxford, 1963.
11. Uesaka, H.; Kobayashi, R. J Cryst Growth 2002, 237–239, 132.
12. Rossi, B. Optics; Addison–Wesley Publishing Co.: Reading, MA, 1967.
13. Iwatsubo, T.; Kusmocahyo, S. P.; Sinbo, T. J Appl Polym Sci 2002, 86, 265.